Characteristics of Pristine Carbon Nanotube & Graphene Field Effect Transistors

Carbon Nanotube Network Morphology

Figure 1 shows a side-by-side comparison of the surface morphology of carbon nanotube films fabricated using the methods described in **?@sec-dep-carbon-nanotubes**. These images were collected using an atomic force microscope and processed in the manner described in **?@sec-afm-characterisation**. They each show bundles of carbon nanotubes with a range of diameters and lengths, with each bundle containing one or multiple nanotubes. As discussed in previous works using solvent-based deposition techniques for depositing carbon nanotubes, multi-tube bundles form due to strong mutual attraction between nanotubes [@Zheng2017; @Thanihaichelvan2018; @Thanihaichelvan2019; @Nguyen2021]. However, when surfactants are present, they adsorb onto the carbon nanotubes and form a highly repulsive structure able to overcome the strong attraction between nanotubes. This repulsion then keeps the individual carbon nanotubes isolated [@Wenseleers2004; @Shimizu2013]. The diameter range provided by the supplier for the individual carbon nanotubes used is $1.2 - 1.7$ nm, while the length range is $0.3 - 5.0$ μm (Nanointegris).

The distribution of the deposited carbon nanotubes was modelled to quantatively understand the effect of the various methods used on the resulting network morphology. The diameter range of deposited single-walled carbon nanotubes can be modelled via a normal or Gaussian distribution [@Thanihaichelvan2018; @Liu2013; @Vobornik2023]. However, when we extract and bin the height profiles from the 2.5 μm $\times$ 2.5 μm AFM images in Figure 1, the histograms do not follow a normal distribution. The AFM histogram shape results from the SiO_2 substrate and carbon nanotubes both exhibiting a degree of surface roughness, which is partially due to the presence of atmospheric contaminants. In the case of the surfactant-deposited networks, residual surfactant may also contribute to surface roughness [@Vobornik2023].

It has been demonstrated that the surface roughness of a bare SiO_2 substrate can also be modelled with a normal distribution. This normal distribution has a spread of approximately ± 1 nm about the mean, which can be set as the reference or zero point for other height measurements [@Velicky2015]. As both the carbon nanotube and silicon dioxide background heights can each be modelled using a normal distribution, we therefore assume that a linear combination of normal distributions can be used to model the AFM histograms in Figure 1.

By using the analysis discussed in **?@sec-histogram-analysis**, we find that a linear combination of normal distribution fits to all histograms corresponding to the AFM images in Figure 1 with an R-squared value of at least 0.987. The first or left-most distribution for all three figures in Figure 2 corresponds to the SiO_2 substrate roughness, centered at ~ 0 nm

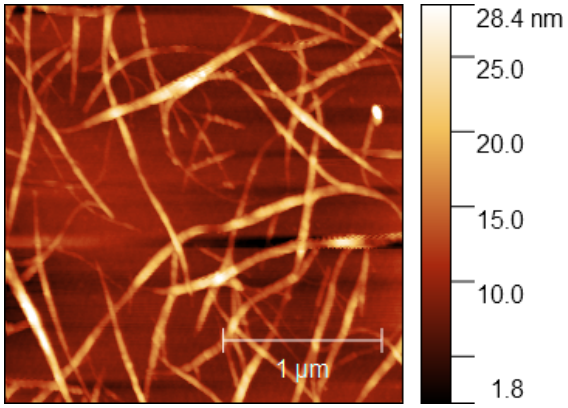

(a) Solvent-based deposition

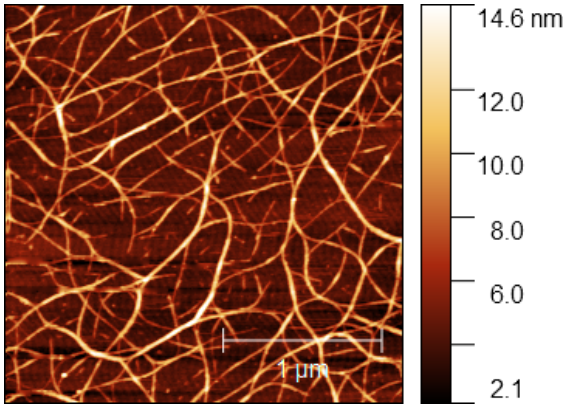

(b) Dropcast surfactant-based deposition

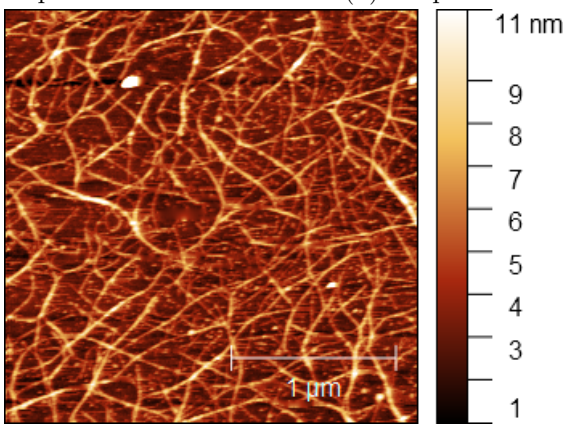

(c) Steam-assisted dropcast surfactant-based deposition

Figure 1: 2.5 μm $\times$ 2.5 μm atomic force microscope images of carbon nanotube films deposited using various methods. NOTE NEED TO ADD EXAMPLES OF SURFACTANT BASED DEPOSITION POST-ANNEALLING!!!

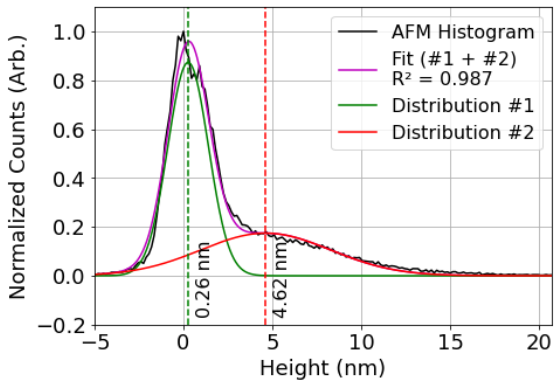

(a) Solvent based deposition

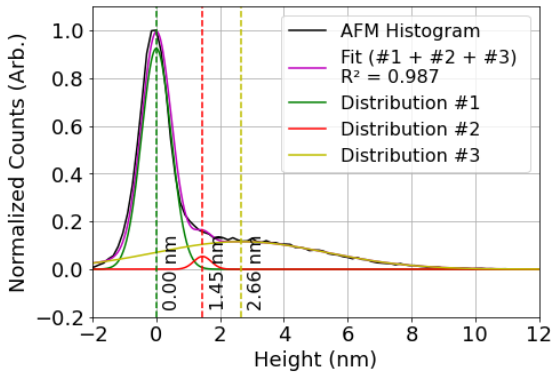

(b) Dropcast surfactant-based deposition

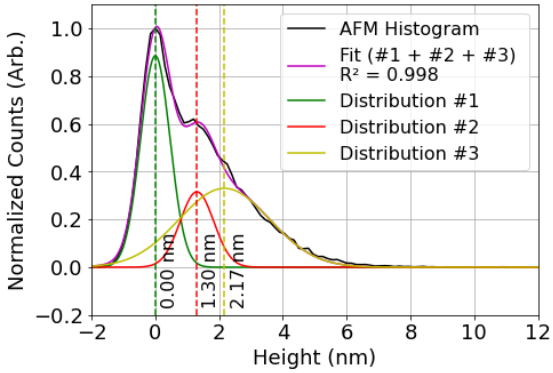

(c) Steam-assisted dropcast surfactant-based deposition

Figure 2: Surface profile histograms extracted from the 2.5 μm $\times$ 2.5 μm atomic force microscope images seen in Figure 1, each fitted with a linear combination of normal distributions. The component normal distributions corresponding to each linear combination are also shown.

and with a standard deviation of $0.4 - 1.2$ nm. For the carbon nanotube film deposited with solvent, the second distribution then corresponds to bundles of carbon nanotubes. If we model bundles as cylinders, and we assume the component nanotubes follow 2D packing and are of equal diameter, we can give an estimate the mean bundle size in terms of number of nanotubes n [@Graham1998; @Thanihaichelvan2018; @Specht2023].

```
#|

knitr::opts_chunk$set(echo = FALSE)
library(knitr)
library(kableExtra)

circle_packing <- read.csv("tables/ch5/circle_packing.csv", sep=",")
circle_packing <- circle_packing[rowSums(is.na(circle_packing)) == 0,]

knitr::kable(circle_packing, col.names = NULL, format = "simple")
```

Table 1: The first eight optimised ratios of 2D packed circle diameter to encompassing circle diameter, given to 3 s.f. (encompassing circle diameter = d, number of packed circles = n, approximate packed circle diameter = d_n).

n	2	3	4	5	6	7	8	9
d/d_n	2.00	2.15	2.41	2.70	3.00	3.00	3.30	3.61

Table 1 shows the relationship between the diameter of a bundle and the constituent diameters of up to nine 2D packed carbon nanotubes within that bundle. The second distribution in Figure 2a indicates the mean diameter of carbon nanotube bundles is 4.62 nm. Assuming an average carbon nanotube diameter of 1.45 nm, we find a d/d_n packing ratio of 3.19, indicating an average bundle composition of ~ 7 nanotubes in Figure 2a.

For the carbon nanotube networks deposited using surfactant in Figure 2, we notice that there are two non-SiO_2 distributions present. The mean of the second distribution, the left-most non-SiO_2 distribution, falls below the average height for a single carbon nanotube. This attribute indicates that the distribution either represents broken pieces of individual carbon nanotubes, residual surfactant or other atmospheric contamination resistant to acetone and isopropanol rinsing. This contamination distribution is significantly larger for the carbon nanotube devices which used steam in the deposition process. The presence of this contamination histogram distribution was consistently found for all sampled surfactant-deposited film AFM data, while not present for any of the sampled solvent-deposited films.

From Figure 1c, we also see that steam deposited devices have sparsely distributed ~ 10 nm high features visible on their surface which are not present for the other films. These

Table 2: The mean of histogram distributions across three different samples for carbon nanotube films deposited using various methods, along with the mean sample coverage with bundles and mean proportion of multitubed bundles present. The mean of the carbon nanotube bundle distribution is shown with an estimate of the number of nanotubes that could pack into the mean bundle size via 2D packing.

	Distribution Mean (nm)			**Bundle Attributes**	
	Silicon	Contaminant	Bundles (tubes)	% multi-tube	% coverage
Solvent deposited	0.1 ± 2.3	—	6.2 ± 3.7 (13)	78 ± 16	35 ± 21
Surfactant deposited	0.0 ± 0.4	1.0 ± 0.4	2.0 ± 1.8 (1)	27 ± 25	31 ± 9
Surfactant deposited with steam	0.0 ± 0.5	1.3 ± 0.6	2.0 ± 1.2 (1)	17 ± 17	50 ± 11

observations may be evidence of trapped water microdroplets on the surface from the steam, or could be from the steam causing surfactant to form persistent features on the surface. The size of this central peak may be useful for determining the extent of contamination in a carbon nanotube film, discussed further in **?@sec-contamination**. Such contamination may or may not have implications for biosensing suitability, but surfactant contamination could certainly have negative effects on biological elements sensitive to surfactant.

The distribution means corresponding to each type of deposition method, averaged across histogram fits from three 2.5 μm × 2.5 μm atomic force microscope images, are given in Table 2. The carbon nanotube bundle mean is given alongside the number of carbon nanotubes corresponding to the mean height according to 2D packing as given in Table 1 and Thanihaichelvan *et al.* [@Thanihaichelvan2018].

It is noticeable that the location of silicon and contamination distribution means are highly consistent between films. Also notable is a the large decrease in bundle size when surfactant is used in the deposition process. There is also a large standard deviation in mean bundle size seen for solvent deposited devices, corresponding to a wide range of bundle sizes present on the atomic force microscope images of the solvent-deposited films.

It is also important to consider that for all figures in Figure 1, larger height measurements in the carbon nanotube distribution include surface contamination on the carbon nanotubes as well as bundle-bundle junctions. The distribution may also encompass broken nanotube pieces and some silicon oxide surface contamination at the low end of the range. When considering the proportion of single-tube bundles relative to multi-tube bundles, we exclude heights from the carbon nanotube normal distribution below 1.2 nm, the minimum height of the supplied

carbon nanotubes. We also exclude heights above double the distribution mean, to ignore bundle-bundle junctions and surface contamination.

We then compare the proportion of the curve below and above 2.9 nm, the minimum multi-tube bundle size for 1.45 nm diameter nanotubes. By doing so, we get a rough estimate of the proportion of single- to multi-tube bundles present on the surface. We can also compare the total area of the carbon nanotube distribution to the area of the other distributions to get an estimate of the surface coverage by bundles. These values, averaged across the histogram fits from three 2.5 μm $\times$ 2.5 μm atomic force microscope images, are given in Table 2. It should also be noted that nanotubes undergo some compression from the AFM tip, so these values are possibly underestimates. However, the mean values for surfactant-deposited films are in line with those previously found for IsoNanotubes-S deposited on silicon oxide using alternative analysis methods [@Vobornik2023].

In Figure 1 and Table 2, we see that carbon nanotubes deposited in a surfactant dispersion form bundles which are significantly less wide than the bundles in the film deposited using solvent. However, we also see that despite the presence of surfactant, not all surfactant-dispersed carbon nanotubes are deposited individually. Bundling may occur during the process of deposition onto the substrate, which could disrupt the repulsive forces from the surfactant coating and allow attractive forces to temporarily dominate. The

It is possible that the bundling of surfactant-dispersed carbon nanotubes occurs due to the coffee-ring effect [@Deegan1997; @VanGaalen2021]. The coffee-ring effect refers to a build-up of dispersed solid forming around the edges of a dispersion evaporating on a surface. This process occurs due to the dispersion edges being fixed by surface forces, leading to capillary flow outwards to replace liquid evaporating at the edges, bringing solid material along with it. The presence of vapour is known to disrupt this effect [@Bishop2020]. Table 2 demonstrates that on average, the presence of steam reduces the number of nanotube bundles present and increases surface coverage, supporting the above hypothesis.

Electrical Characteristics

Carbon Nanotubes

Each carbon nanotube device fabricated was electrically characterised as described in **?@sec-electrical-characterisation**. Figure Figure 3 displays multi-channel measurements of representative devices fabricated as described in **?@sec-fabrication**. To ensure a consistent comparison, each device here was encapsulated with AZ® 1518 encapsulation before measurements were taken. The channels which did not exhibit reliable transistor characteristics are not shown. These non-working channels were either short, due to metal remaining on the channel after lift-off, or were very low current, due to a very sparse carbon nanotube network. Devices shown here with a solvent-deposited carbon nanotube network were fabricated prior to Jan 2022; devices with a surfactant-deposited network without steam present were fabricated

prior to Jun 2021; devices with a surfactant-deposited network without steam were fabricated prior to Sep 2022.

Consistent subthreshold regime behaviour between channels is desirable for reliable multiplexed biosensing.

Salt Concentration Sensing with Phosphate Buffered Saline

-nLOF2020 resist being used leads to devices with less drift!!

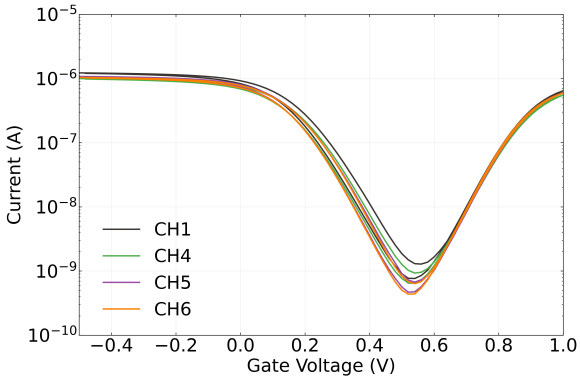

(a) Solvent-based deposition, back-gated

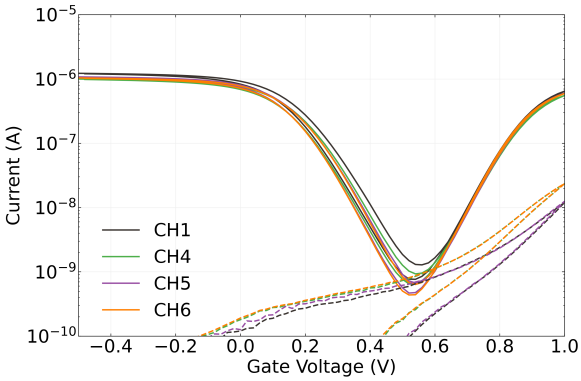

(b) Solvent-based deposition, aqueous-gated

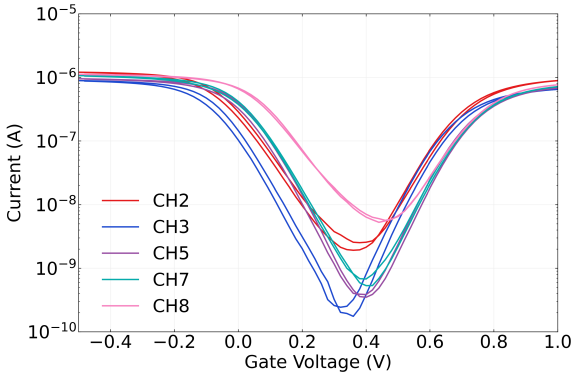

(c) Dropcast surfactant-based deposition, back-gated

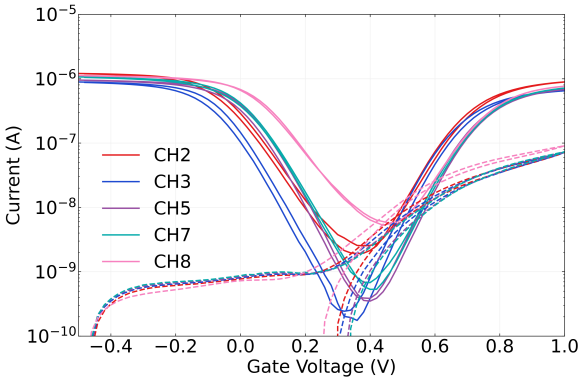

(d) Dropcast surfactant-based deposition, aqueous-gated

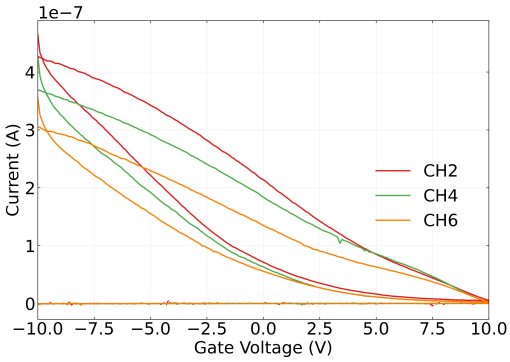

(e) Steam-assisted dropcast surfactant-based deposition, back-gated

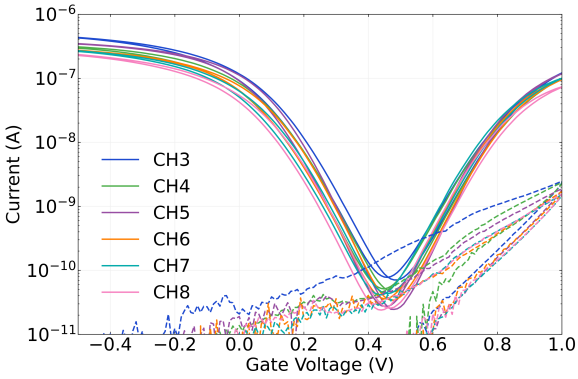

(f) Steam-assisted dropcast surfactant-based deposition, aqueous-gated

Figure 3: Transfer characteristics of carbon nanotube networks deposited using various methods. 1XPBS was used as the buffer for the liquid-gated measurements here. Source-drain voltage used was $V_{ds} = 100$mV, with a step size of either 10 or 20 mV used for the sweep.